Gradient-Based Combined Structural and Control Optimization

David F. Miller* and Jaedong Shim†
Wright State University, Dayton, Ohio

This paper considers the combined structural and control optimization problem for flexible systems. The sum of structural mass and controlled system energy terms is minimized simultaneously in structural and control parameters using gradient searches. The purpose of control is to effectively suppress structural vibrations due to initial excitations. Starting with a baseline structural design, the objectives of the combined structural/control optimization are twofold: 1) to reduce the structure's mass, and 2) to reduce total system strain, kinetic and control energies observed when the structure is excited. The appropriate weighting of energy and structural mass for balanced design and the dependence of optimal designs on initial conditions are discussed. The ideas presented are illustrated through numerical simulations using a 10-bar cantilevered truss.

I. Introduction

CONSIDERABLE interest has been generated recently in the possibility of simultaneously optimizing structural and control designs for flexible systems.[1-10] This concept was given a precise problem formulation in Refs. 2-4 as the joint minimization, in structural parameters and control variables, of a performance criterion consisting of the sum of structural mass and the quadratic performance index associated with the linear regulator optimal control problem. System dynamics were permitted to depend explicitly on structural parameters, a key idea in this and all other related formulations. The necessary conditions for minimizing this criterion subject to the dynamics satisfying fixed initial and terminal conditions were derived using the calculus of variations.

Ref. 7 considers the fixed endpoint linear regulator problem in modal space for parameter-dependent structural systems. Optimal control theory provides the optimal control for each choice of structural parameters. Minimization in structural parameters is accomplished using a gradient projection optimization. Ref. 6 presents an eigenspace optimization approach to the dual structural/control design problem. Based upon a continuation procedure, it permits the minimization of a general performance measure which is a function of a structural parameter vector and the corresponding system eigenvalues and eigenvectors. Constraints are imposed which are also explicit functions of these three quantities.

Ref. 10 considers the simultaneous minimization, in structural and control variables, of the sum of structural mass and the infinite horizon linear regulator quadratic control cost. It is shown that the problem reduces to a minimization over the structural variables alone since optimal controls are always determined through the solution of specified algebraic Riccati equations. It is observed that the derivatives (with respect to structural parameters) of the Riccati equation solutions satisfy Lyapunov equations. The Newton-Raphson (second-order) algorithm proposed for the solution of the Kuhn-Tucker optimality conditions centers about these derivatives.

The purpose of this study is to further explore the computational feasibility of the combined structural/control design concept as applied to vibration suppression in structural systems. Specifically, we focus upon the problem formulation of Ref. 10 previously described. Given an initial structural design, the objective of our optimization is to reduce *both* the mass *and* the vibrational energy at the *same time*. Constraints are imposed on structural parameters by restricting system natural frequencies and the sizes of structural elements. Control is provided by the optimal feedback gains of linear regulator theory. Optimization in the structural parameters is accomplished using gradient projection and penalty function techniques, thus avoiding the need for costly second-derivative computations.

The optimization strategy developed is applied to the 10-bar cantilevered truss of Ref. 11. Simulations are performed by linking finite-element, control, and structural parameter optimization programs into a single, integrated package for the purpose of updating models, computing structural derivatives, and determining optimal controls and structural parameter improvements. The analysis is formulated and conducted in a general finite-element setting and hence is applicable in theory to flexible system models of high dimension.

II. Optimization Problem

Consider a dynamic system governed by

$$M(\xi)\ddot{r}+C(\xi)\dot{r}+K(\xi)r=B_0(\xi)u$$

$$r(0)=r_0, \qquad \dot{r}(0)=\dot{r}_0 \tag{1}$$

where r is an $n\times 1$ vector of physical coordinates (nodal displacements), ξ is a $p\times 1$ vector of structural parameters, u is an $m\times 1$ control vector, and $M(\xi)$, $C(\xi)$, $K(\xi)$, and $B_0(\xi)$ are the mass, damping, stiffness, and control influence matrices of appropriate dimensions, respectively. As usual, we assume that $M(\xi)$ is symmetric, positive definite and $K(\xi)$ is symmetric, positive semidefinite. Formulated in the state space, Eqs. (1) become

$$\dot{x}=A(\xi)x+B(\xi)u$$

$$x(0)=x_0(\xi) \tag{2}$$

where

$$A=\left[\begin{array}{c|c} 0 & I \\ \hline -M^{-1}K & -M^{-1}C \end{array}\right]$$

$$B=\begin{bmatrix} 0 \\ M^{-1}B_0 \end{bmatrix}, \qquad x=\begin{bmatrix} r \\ \dot{r} \end{bmatrix} \tag{3}$$

As in Eq. (3), the vector ξ will often be suppressed for notational convenience. The explicit dependence of x_0 upon ξ will be discussed in Sec. V.

Received March 17, 1986; revision received Aug. 25, 1986.

*Associate Professor, Department of Mathematics and Statistics. Member AIAA.
†Graduate Research Assistant, Department of Mathematics and Statistics.

Consider the minimization of

$$F(\xi,u)=q_1W(\xi)+\tfrac{1}{2}q_2\int_0^\infty[x^TQ(\xi)x+u^TR(\xi)u]\,dt \tag{4}$$

subject to constraints

$$g_j(\xi)\geq G_j, \qquad j=1,2,\ldots,\ell \tag{5}$$

Here the weighting matrices $Q(\xi)$ and $R(\xi)$ are assumed positive semidefinite and positive definite, respectively, $q_1>0$, $q_2>0$ are scalar weights, the $g_j(\xi)$ are functions of ξ, and the G_j are constants. The minimization is to take place simultaneously in ξ and u. For fixed ξ, let $P=P(\xi)$ be the solution of the matrix Riccati equation

$$A^TP+PA+Q-PBR^{-1}B^TP=0 \tag{6}$$

and let

$$u(\xi)=-R^{-1}(\xi)B^T(\xi)P(\xi)x \tag{7}$$

be the corresponding optimal control from linear regulator theory. If (ξ^*,u^*) minimizes F subject to Eq. (5), then fixing $\xi=\xi^*$ in Eq. (4), it is easily seen (cf. Ref. 10) that u^* may be taken to be the optimal control $u(\xi^*)$ defined through Eq. (7). Thus, the minimization of F reduces to minimizing, in ξ alone,

$$J(\xi)=F(\xi,u(\xi))=q_1W(\xi)+\tfrac{1}{2}q_2x_0^T(\xi)P(\xi)x_0(\xi) \tag{8}$$

for the given initial condition $x_0(\xi)$. The integral in Eq. (4) is expressed in terms of x_0 and P using standard optimal control theory.

III. Solution Technique

For numerical optimization purposes, ∇J is required. A computation shows that

$$J_{\xi_i}=\frac{\partial J}{\partial\xi_i}=q_1W_{\xi_i}+\tfrac{1}{2}q_2x_0^TP_{\xi_i}x_0+q_2x_0^TPx_{0,\xi_i} \tag{9}$$

where P_{ξ_i} satisfies the Lyapunov equation

$$[A^T-PBR^{-1}B^T]P_{\xi_i}+P_{\xi_i}[A^T-PBR^{-1}B^T]^T$$
$$+[A_{\xi_i}^TP+PA_{\xi_i}-P(BR^{-1}B^T)_{\xi_i}P+Q_{\xi_i}]=0 \tag{10}$$

Here x_{0,ξ_i} denotes $(\partial/\partial\xi_i)x_0(\xi)$. Equation (10) requires R to be symmetric. Note that $(x_{0,\xi_i}^TPx_0)^T=x_0^TPx_{0,\xi_i}$ since P is symmetric.

To minimize J subject to Eq. (5), Ref. 10 proposes an iterative solution, based upon Newton's method, of the appropriate Kuhn-Tucker optimality conditions. (In Ref. 10, $x_0(\xi)\equiv x_0$ is independent of ξ.) This solution requires the calculation of the mixed partial derivatives $J_{\xi_i\xi_j}$. From Eq. (9) $J_{\xi_i\xi_j}$ depends upon $P_{\xi_i\xi_j}$. Differentiating Eq. (10), one sees that $P_{\xi_i\xi_j}$ satisfies a Lyapunov equation involving mixed partials of A,B,Q, and R. In order to avoid the expense of computing second derivatives (especially for high-order systems), this paper explores the use of the method fo steepest descents to minimize J. When constraints are present, the augmented function

$$\hat{J}(\xi)=q_1W(\xi)+\tfrac{1}{2}q_2x_0^T(\xi)P(\xi)x_0(\xi)+\Sigma_jr_j(\xi)[g_j(\xi)-G_j]^2 \tag{11}$$

is minimized. Here the penalty multiplier $r_j(\xi)$ is given by

$$r_j(\xi)=\begin{cases}0 & \text{if } g_j(\xi)\geq G_j\\ c & \text{if } g_j(\xi)<G_j\end{cases} \tag{12}$$

where $c>0$ is a chosen constant.

Recall that in theory, as $c\to\infty$, the corresponding ξ values minimizing $\hat{J}$ in Eq. (11) converge to a value ξ^* that minimizes J in Eq. (8) subject to the constraints of Eq. (5). If constraints such as $\omega_j(\xi)\geq\bar{\omega}_j$ are imposed ($\bar{\omega}_j>0$ constant) on the open loop frequencies $\omega_j(\xi)$ of Eq. (2), analytical derivatives $\omega_{j,\xi_i}(\xi)$ must be computed to determine $\nabla\hat{J}=(\hat{J}_{\xi_1},\hat{J}_{\xi_2},\ldots,\hat{J}_{\xi_p})^T$. As is well known,[12]

$$\frac{\partial}{\partial\xi_i}\omega_j^2=2\omega_j\omega_{j,\xi_i}=\frac{1}{\phi_j^TM\phi_j}\left[\phi_j^T(K_{\xi_i}-\omega_j^2M_{\xi_i})\phi_j\right] \tag{13}$$

where the $\omega_j^2=\lambda_j$ and corresponding vectors ϕ_j are solutions of the eigenvalue problem

$$K\phi_j=\lambda_jM\phi_j \tag{14}$$

If simple magnitude constraints $\xi_j\geq\bar{\xi}_j$ are imposed, $J(\xi)$ in Eq. (8) may be minimized straightforwardly using the gradient projection technique.

IV. 10-Bar Truss and Computational Strategy

Consider the 10-bar cantilevered truss of Fig. 1. Base nodes 5 and 6 are held fixed, while nodes 1–4 are free. A finite-element model (1) is employed to describe the in-plane dynamics of this two-dimensional structure. For simplicity, it is assumed that $C=0$. The variables r_1–r_8 measure the relative x and y (horizontal and vertical) displacements of nodes 1–4 off their equilibrium positions (e.g., r_5 and r_6 are the x and y displacements of node 3). The truss is assumed to be constructed of aluminum, with the following physical dimensions and material properties (cf. Ref. 11):

Length	= 100 in.
Base width	= 36 in.
Tip width	= 24 in.
Modulus of elasticity	= 10^7 lb/in.^{2}
Weight density	= 0.1 lb/in.^{3}

In addition, a nonstructural mass of 1.29 lb-s^2/in. is assumed to be present at each of the nodes 1–4. (In all cases considered below, the nonstructural mass is much greater than the structural mass.)

For motion (vibration) control, accuators are assumed to be located at nodes 1–4. The parameter vector $\xi=(\xi_1,\xi_2,\ldots,\xi_{10})^T$ is chosen with ξ_i measuring the cross-sectional area of bar i of the truss, $i=1,2,\ldots,10$. For symmetry, it is assumed that $\xi_1=\xi_3$, $\xi_4=\xi_6$, $\xi_7=\xi_8$, and $\xi_9=\xi_{10}$. An initial (baseline) design ξ_0 is characterized by setting $\xi_i^0=0.1$ in^2 for all i. Excluding nonstructural mass, the resulting truss weighs 4.88 lb.

This paper presents numerical results for the solution of the combined structural and control optimization problem, as discussed in Secs. II and III, for the 10-bar truss. The control objective is the suppression of structural vibrations resulting from initial excitations x_0. We attempt to minimize J in Eq. (8) by minimizing $\hat{J}$ in Eq. (11) (omit the penalty terms when constraints are absent). The function $W(\xi)$ is always taken to be the mass of the truss specified by the vector ξ, excluding the nonstructural mass. The function $x_0^TPx_0$ is determined by Q and R. From a structural dynamicist's point of view, natural choices for Q and R are (see Ref. 11)

$$Q(\xi)=\begin{bmatrix}K(\xi) & 0\\ 0 & M(\xi)\end{bmatrix} \text{ and } R(\xi)=B_0^T(\xi)K(\xi)^{-1}B_0(\xi) \tag{15}$$

With these choices, $x_0^TPx_0$ in Eq. (8) provides a measure of total system strain, kinetic and control energies. We employ the matrices in Eq. (15) in this study. Loosely speaking then, given a baseline truss design ξ^0, the goal of optimization here is to identify a less massive design ξ^* with reduced total controlled system energy content.

To minimize $\hat{J}$ for a given initial vector ξ^0, $-\nabla\hat{J}$ is employed to generate a sequence $\xi^1, \xi^2, \ldots$ with $\hat{J}(\xi^{k+1}) < \hat{J}(\xi^k)$ and hopefully $\hat{J}(\xi^k) \to \hat{J}(\xi^*)$. The minimization of $\hat{J}$ is accomplished by linking together 3 computer programs: 1) a finite-element program, 2) an optimal control program, and 3) an optimization/driver program. Program 1 is employed to construct models in the form of Eq. (2) for given parameter vectors ξ. Program 2 solves Eq. (6) and evaluates $x_0^T P x_0$. Program 3 computes $\nabla\hat{J}$ by computing derivative of A,B,Q, and R and then solving Eq. (10). This program also computes derivatives of the g_j as needed and coordinates the use of programs 1) and 2) in implementing the steepest descents optimization. The derivatives of A,B,Q, and R depend on the derivatives of M,K, and B_0. For the 10-bar truss, these later derivatives are constant. For general finite-element models, derivatives may be computed either explicitly, by taking advantage of the special structure in the models considered, or numerically, using finite-difference approximations. For a more thorough description of the specific features of the algorithm employed, the reader is referred to Ref. 9.

V. Initial Conditions and q_1, q_2 Selection

We now begin our discussion of simulation results for the 10-bar truss. Concisely, our problem is: minimize J in Eq. (8) subject to Eq. (5) (via the minimization of $\hat{J}$) with Q and R as in Eq. (15) and $\xi_i^0 = .1$ for all i. We consider two initial conditions (structural excitations) $x_0 = [r(0)\ \dot{r}(0)]^T$, denoted $x_0^1(\xi)$ and $x_0^2(\xi)$. In both cases, the displacements $r_i(0)$ are set equal to the equilibrium displacements observed in the truss when statically loaded at nodes 1-4. We set the velocities $\dot{r}_i(0) = 0$ for all i. Since structural characteristics and hence static displacements depend upon ξ, so does $x_0 = x_0(\xi)$. Specifically, $x_0 = x_0^1(\xi)$ is determined when 10,000 lb of force is applied (upward) at nodes 1-4, and $x_0 = x_0^2(\xi)$ is determined when the forces at nodes 3 and 4 in 1 are reversed (applied downward). If the truss is viewed as a cantilevered beam, x_0^1 and x_0^2 are chosen to excite modes 1 and 2, respectively.

Since J is the weighted sum of structural mass and energy, which are noncommensurate quantities, a question arises as to the physical meaning of its minimization. In this paper, we are not concerned with providing a precise interpretation of J. Rather, we are concerned with using J to achieve the earlier stated goal of reducing W and $x_0^T P x_0$ *simultaneously*. We accomplish this by selecting q_1 and q_2 appropriately. The comparison of masses W for different truss designs is unambiguous. As for the energy terms, $x_0^T P x_0$ measures the total system energy developed in response to the initial excitation x_0. We can meaningfully compare system energies in different truss designs only if we measure their dynamic responses under the same loading conditions. It is important therefore to permit x_0 to depend upon ξ. Indeed, as is seen in Ref. 9, optimization with x_0 independent of ξ can lead to erroneous conclusions. (It should be remarked that it was recognized early on in the combined structural/control optimization literature that optima depend upon initial conditions, and that initial conditions constitute derived information—i.e., they are derived from applied disturbances. This fact motivated the authors of Refs. 2-4 and 7-8 to consider the problem of fixed endpoint maneuvers. Thus they posed the optimization problem directly in terms of mission requirements, rather than derived characteristics which, as in the case of settling after maneuvers, will vary as the structure is varied. It seems likely however, that optimal designs for fixed endpoint problems also vary with specific chosen endpoint conditions.)

For the examples considered, $x_0^T P x_0$ is between 3 and 4 orders of magnitude greater than W. For a balanced minimization of these terms then, the choices for q_1 and q_2 are clearly important. Factoring q_2 out of J, we may assume that $q_2 = 1$ ($J = q_2[q_1/q_2 W + \frac{1}{2}x_0^T P x_0]$) since only the ratio q_1/q_2 determines ξ^*. As expected, experimentation reveals that in general, for large q_1 values, the minimization of W dominates the minimization of J. Decreases in W are accompanied by increases in $x_0^T P x_0$. All bar thicknesses decrease, while the initial vertical displacements of nodes 1-4 increase. Conversely, for small q_1 values, $x_0^T P x_0$ decreases while W increases. Correspondingly, bar thicknesses increase, leading to decreased initial nodal displacements.

Data for the specific cases considered in this study is recorded in Table 1. In each case, optimal ξ_i values are listed along with percentage decreases in W and $x_0^T P x_0$. These changes are measured with respect to the corresponding W

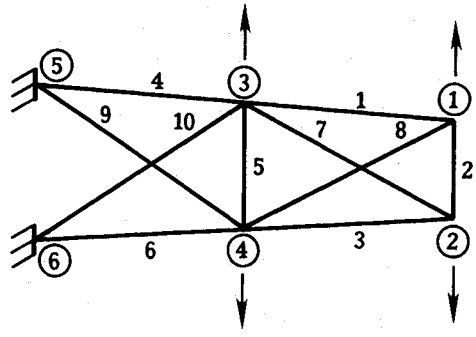

Fig. 1 10-bar cantilevered truss.

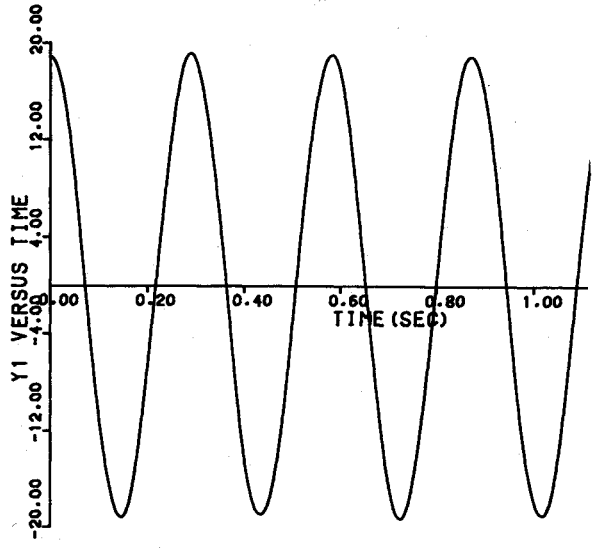

Fig. 2 Uncontrolled node 1 displacements—$\xi_i = .1$, all $i, x_0 = x_0^1$.

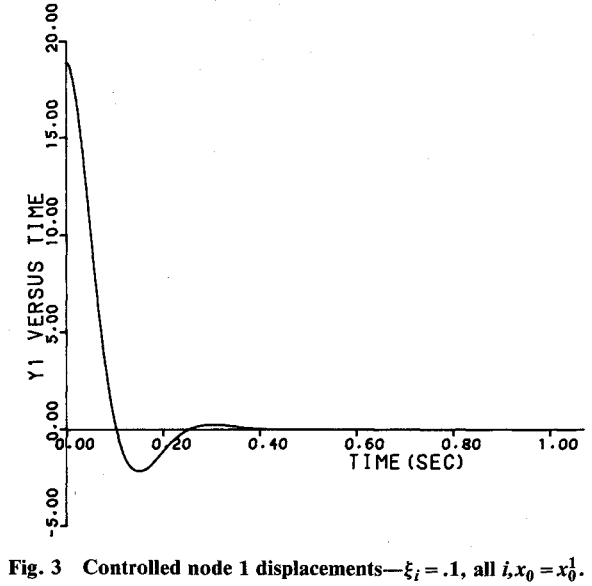

Fig. 3 Controlled node 1 displacements—$\xi_i = .1$, all $i, x_0 = x_0^1$.

and $x_0^T P x_0$ values for the baseline design $\xi_i^0 = .1$, all i, excited with the same initial condition x_0^1 or x_0^2. Minimal and maximal system open- and closed-loop frequencies (in rad/s) are included in Table 1, and the choices of initial conditions and constraints are indicated. Constraints on the ξ_i and $\omega_1(\xi)$, the fundamental truss open-loop frequency, are considered. The "optimal" q_1 values listed in Table 1 were selected roughly as those which permitted reasonable simultaneous unconstrained reductions of both W and $x_0^T P x_0$ for given excitation $x_0(\xi)$ (see cases I and II, Table 1). These selections were made somewhat subjectively. Exhaustive searches over the possible q_1 values were prohibited by the associated high computational costs. (Unfortunately, optimal q_1 values generally change with each specific example considered and determining them represents an additional computational expense.) The data listed in Table 1 give an indication of the degree of design improvement possible through this analysis. A discussion of each of the cases follows.

VI. Simulation Results

Cases I and II present the unconstrained minimization J for the initial conditions $x_0^1(\xi)$ and $x_0^2(\xi)$, respectively. Note the differences in the optimal ξ_i values for these cases. (To prevent any ξ_i from being driven to zero, lower bounds $\xi_i \geq .0001$ were imposed in all computations.) This data demonstrates graphically the dependence of ξ^* upon the initial data x_0 (i.e., the loading which produces x_0). This is a very important point that bears emphasizing. Unlike the optimal feedback control for the linear regulator problem which is independent of initial conditions, in general, for the minimization of J, ξ^* *will vary with* x_0.

Constraints are imposed in cases III–VI. It should be remarked that for the constrained minimization problems considered in this study, the effectiveness of $\hat{J}$ as an optimization criterion was disappointing. In theory, ξ^* can be determined by letting the penalty constant $c \to \infty$. In practice however, as c

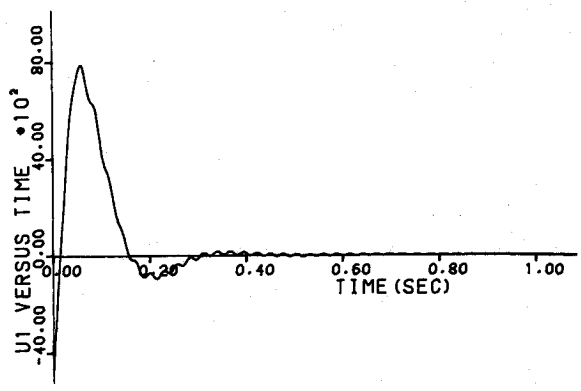

Fig. 4 Accuator inputs at node 1—$\xi_i = .1$, all $i, x_0 = x_0^1$.

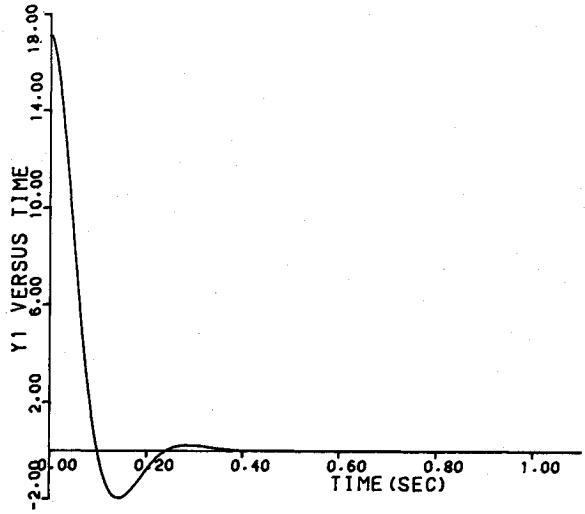

Fig. 5 Node 1 displacements—case III, $.05 \leq \xi_i \leq .15$, $x_0 = x_0^1$.

Table 1 Optimization results for the 10-bar truss

Case	Baseline		I	II	III	IV	V	VI	VII	VIII	IX
x_0	$x_0^1(\xi)$	$x_0^2(\xi)$	$x_0^1(\xi)$	$x_0^2(\xi)$	$x_0^1(\xi)$	$x_0^2(\xi)$	$x_0^1(\xi)$	$x_0^2(\xi)$	$x_0^1(\xi)$ Min W	$x_0^1(\xi)$	$x_0^1(\xi)$
q_1			3850	1500	3850	1500	3850	1500	$p = .0005$	3850	3850
Constraints			None	None	$.05 \leq \xi_i \leq .15$	$.05 \leq \xi_i \leq .15$	$\omega_1 \leq 22.9$	$\omega_1 \geq 20.0$	$\omega_1 = 21.6$	$\xi_i^0 = .05$	$\xi_i^0 = .15$
$\xi_1 = \xi_3$		.1	.05274	.07829	.05254	.07587	.09374	.08197	.05499	.05453	.06475
ξ_2		.1	.01104	.08312	.05000	.05087	.09757	.08629	.07792	.00433	.06366
$\xi_4 = \xi_6$		.1	.18586	.14654	.15000	.15000	.12284	.14425	.14666	.18527	.18690
ξ_5		.1	.00010	.07893	.05000	.05000	.09697	.08289	.07244	.00010	.04228
$\xi_7 = \xi_8$		.1	.06076	.08112	.06657	.08050	.09384	.08444	.05680	.05973	.06573
$\xi_9 = \xi_{10}$		.1	.08367	.00835	.08860	.05000	.09746	.02682	.05701	.07877	.08644
Decrease in $W(\xi)$			15.7%	24%	15.6%	17%	−1%	18%	23%	17.3%	6%
Decrease in $x_0^T(\xi)P(\xi)x_0(\xi)$			24%	32%	15.1%	20.8%	16.3%	26.8%	−5%	22%	30%
Decrease in $J(\xi)$			18.8%	26%	15.4%	18.2%	5.5%	20.5%		19%	14.9%
Min. open loop frequency, (rad/s)	21.6		23.5	13.8	22.6	22.4	23.0	20.0			
Max. open loop frequency	275		237	253	231	246	271	258			
Min. closed loop frequency	21.2		23	13.5	22.1	21.9	22.5	19.6			
Max. closed loop frequency	257		237	236	229	243	256	241			
Initial node 1 displacement, in.	18.9	10.0	15.8	5.8	17.1	8.5	16.8	7.8			
Max. node 1 accuator input, pounds force	7900	4300	7500	5800	7800	4500	8000	5200			

increases, one finds it increasingly difficult to complete successful steps (ones that decrease $\hat{J}$) away from ξ^0. Thus, one attempts to choose an "optimal" $c>0$, one sufficiently large so that the constraints are approximately satisfied, and at the same time, the steepest descents algorithm is able to select a sequence ξ^k with $\hat{J}(\xi^k)$ decreasing. Although this strategy can be made to work here, the selection of c is a time-consuming and frustrating process. Fortunately, as described below, we were usually able to bypass $\hat{J}$ and minimize J directly.

In cases III and IV, constraints $.05 \le \xi_i \le .15$ are imposed. In these cases, J is most easily minimized by projecting ∇J onto the tangent subspace of the feasible region determined by the active constraints. (As a practical matter, the ξ_i are observed to increase or decrease monotonically as the minimization proceeds so that once ξ_i reaches .05 or .15, it remains there.) The excessively small ξ_i values of cases I and II are now absent (see Table 1), while still impressive reductions in mass and energy are observed.

In cases V and VI, the constraints $\omega_1(\xi) \le 22.9$ rad/s (3.64 Hz) and $\omega_1(\xi) \ge 20.0$ rad/s (3.18 Hz), respectively were imposed. The baseline design $\xi_i^0 \equiv .1$ has $\omega_1(\xi^0) = 21.6$ rad/s (3.44 Hz). For these cases, $\hat{J}$ was minimized with $g_1(\xi) = -\omega_1(\xi)$ and $g_1(\xi) = \omega_1(\xi)$, and $G_1 = -22.9$ and $G_1 = 20.0$, respectively. Consider first case VI, for which $x_0 = x_0^2(\xi)$. For this case, we were able to reduce $\hat{J}$ significantly, but as previously remarked, locating an optimal c value was time-consuming, and the repeated solution of Eq. (14) added to the computational expense. Observing that in case II $\omega_1(\xi)$ decreased monotonically as the algorithm proceeded, to minimize J we tried simply proceeding with steps in the direction $-\nabla J$ until $\omega_1(\xi)$ decreased to 20.0. The resulting ξ^* was then accepted as the optimal design. This stategy worked very well, producing these results in Table 1. Significant reductions in mass and energy are observed. These reductions are comparable to those achieved via the minimization of $\hat{J}$.

If the constraint $\omega_1(\xi) \ge 20.0$ of case VI is considered and $\hat{J}$ is minimized with $x_0 = x_0^1(\xi)$, interestingly, the constraint is always satisfied, since the frequency $\omega_1(\xi)$ *increases* monotonically as the optimization proceeds. The results of this minimization are therefore identical to those of case I. It appears that $x_0^1(\xi)$ opposes the reduction of the fundamental frequency. (Indeed, when the hard constraint $\omega_1(\xi) = 20.0$ is imposed and $\hat{J}$ is minimized with $x_0 = x_0^1(\xi)$, W decreases 15% but $x_0^T P x_0$ *increases* roughly 20%!) Case V considers the minimization of J with $x_0 = x_0^1(\xi)$ subject to the constraint $\omega_1(\xi) \le 22.9$. Taking advantage of the monotonicity of $\omega_1(\xi)$ previously noted, J can be effectively minimized directly by simply stopping the minimization in case I when $\omega_1(\xi) \le 22.9$ is violated. As seen from Table 1, the minimization of J results in a 16.3% reduction in $x_0^T P x_0$, accompained by a 1% increase in W. (Both W and $x_0^T P x_0$ could be decreased by selecting a "better" q_1 value, although $x_0^T P x_0$ would not decrease as significantly.)

Before considering cases V and VI, we attempted to minimize J subject to the hard constraint $\omega_1(\xi) = 21.6$ ($g_1 = \omega_1 \ge 21.6$ and $g_2 = -\omega_1 \ge -21.6$). We were unable to reduce J at all (being unable to reduce $\hat{J}$) except in the special case $q_1 = 1$ and $q_2 = 0$ [i.e., min $W(\xi)$ alone]. For this one case the penalty function approach worked very well, reducing W a significant 23%. This is case VII in Table 1. (When the resulting optimized truss is controlled with initial condition $x_0^1(\xi)$, however, the energy term $x_0^T P x_0$ increases by 5% over the baseline value.)

At this point, it is interesting to compare our results with those of Salama, Hamidi, and Demsetz.[10] In their paper, as discussed earlier, Newton's method was employed to minimize J with constraints for a segmented (3 segments) cantilevered beam, ξ_i measuring the cross-sectional area of segment i. The beam's fundamental frequency ω_1 was constrained to remain constant at its baseline value, determined when all segments had equal cross-sectional areas. The weighting matrices were chosen to be identities. Three minimization problems were considered: 1) minimize $W(\xi)$ alone, 2) minimize $J(\xi)$ with x_0 equal to the baseline beam's first vibrational mode, and 3) minimize $J(\xi)$ with x_0 equal to the baseline beam's second mode. In all cases, optimal ξ^* values were identical, specifying a beam tapered from base to tip. The dependence of ξ^* on x_0 was not observed. The authors note that the frequency constraint appears to numerically dominate the optimization.

In the cases examined here, ξ^* definitely *does* depend on x_0. A general trend toward tapering the truss from base to tip, which we expect intuitively, is also present. Outside bar thicknesses $\xi_4 = \xi_6$ exceed $\xi_1 = \xi_3$ consistently. Inside bar thicknesses $\xi_9 = \xi_{10}$ exceed $\xi_7 = \xi_8$ in cases I, III, and V, while the opposite is true for cases II, IV, and VI. Presumably these later differences can be attributed to the torquing effect of x_0^2. Bars 2 and 5 are approximately equal in all cases except case I. The 10-bar truss possesses a richer geometry than the segmented beam. In particular, load paths for distributing forces are more complicated. It is not surprising therefore that truss optimizations produce results that are less clear cut than those for the cantilevered beam. Indeed, the results of this section suggest that conclusions drawn from the solution of the combined structural and control problem may be ambiguous due to the dependence of ξ^* on x_0. An additional complication is that the ξ^* located by minimizing J may represent only local minima. The data from cases VIII and IX in Table 1 address this concern.

In case VIII, J with $q_1 = 3850$ is minimized without constraints using $x_0 = x_0^1$ and $\xi_i^0 = .05$ for all i. In case IX, $\xi_i^0 \equiv .15$. Comparing the results with case I, essentially the same optimal parameter vectors are discovered as are found in case I. Thus, the existence of local minima does not appear to be a cause for concern here. The differences observed in the ξ^* vectors in the three cases are most likely due to the algorithm's stopping criterion, since near optimality, decreases in J are very slight at each successful step.

The above evidence suggests that in practice, the combined structural and control problem is quite complicated. However, as seen in Table 1, the payoffs obtainable seem unmistakable.

VII. Dynamic Responses

The uncontrolled response of the baseline truss to the excitation $x_0 = x_0^1(\xi)$ is graphed in Fig. 2. Vertical displacements of node 1 off its equilibrium position are plotted vs time. (Recall that for convenience we have set $C = 0$ so that no internal damping is present.) Node 1 oscillates with a frequency of about 3.44 Hz, the truss's fundamental frequency, so that x_0^1 essentially excites only the first mode. Figure 3 shows the controlled response of the baseline truss when $x_0 = x_0^1$, and control is provided by Eq. (7) with Q and R given by Eq. (15). Accuator inputs at node 1 are graphed in Fig. 4. Clearly, the weighting matrix choices in Eq. (15) insure effective control. Truss vibrations are arrested smoothly and rapidly. (It is interesting to note that for all cases considered, closed-loop fre-

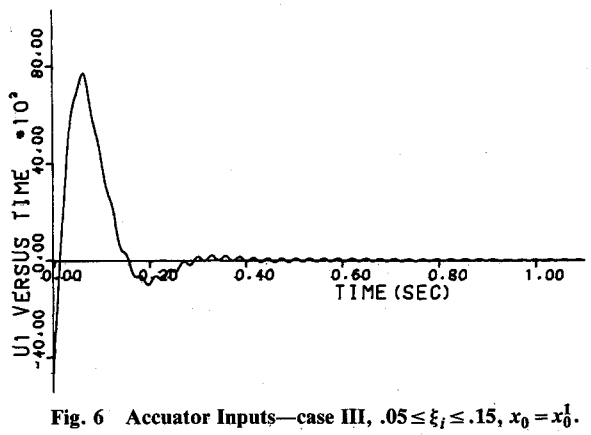

Fig. 6 Accuator Inputs—case III, $.05 \le \xi_i \le .15$, $x_0 = x_0^1$.

Table 2 Optimal $x_0^2(\xi)$ design excited by $x_0^1(\xi)$ (and vice versa); averaged designs; impulse excitation

Case	X	XI	XII	XIII	XIV	XV	XVI	XVII
x_0	$x_0^2(\xi)$	$x_0^1(\xi)$	$x_0^2(\xi)$	$x_0^1(\xi)$	$x_0^1(\xi)$	$x_0^2(\xi)$	$\alpha\cdot\delta(t)$ at node 3 $\alpha=6{,}000$	$\alpha\cdot\delta(t)$ at node 2 $\alpha=2{,}000$
	(Case I)	(Case II)	(Case III)	(Case IV)	(Avg. of cases III and IV)			
$\xi_1=\xi_3$	.05274	.07829	.05254	.07587	.06421	.06421	.07786	.07365
ξ_2	.01104	.08312	.05000	.05087	.05043	.05043	.07702	.10931
$\xi_4=\xi_6$	.18586	.14654	.15000	.15000	.15000	.15000	.09186	.16625
ξ_5	.00010	.07893	.05000	.05000	.05000	.05000	.14348	.07401
$\xi_7=\xi_8$	.06076	.08112	.06657	.08050	.07354	.07354	.03515	.07229
$\xi_9=\xi_{10}$	.08367	.00835	.08860	.05000	.06930	.06930	.14128	.05048
Decrease in $W(\xi)$	15.7%	23.9%	15.6%	17.0%	16.3%	16.3%	9.6%	11.6%
Decrease in $x_0^T(\xi)P(\xi)x_0(\xi)$	4.6%	−392%	−3.9%	1.2%	12.1%	10.0%	9.0%	6.8%
Min. open loop frequency, rad/s	23.5	13.8	22.6	22.4	22.8	22.8	19.3	22.7
Max. open loop frequency	237	253	231	246	238	238	285	273
Min. closed loop frequency	23	13.5	22.1	21.9	22.3	22.3	18.9	22.2
Max. closed loop frequency	237	236	229	243	235	235	278	264
Initial node 1 displacement, in.	9.3	42.0	9.97	17.8	17.0	9.1		
Max. node 1 accuator input, pounds force	4700	6400	4600	7700	7700	4400		

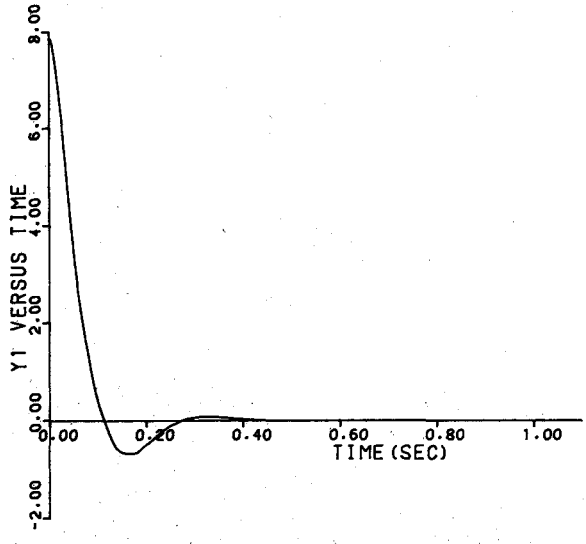

Fig. 7 Node 1 displacements—case VI, $\omega_1(\xi)\geq 20.0$, $x_0=x_0^2$.

quencies are very close to corresponding open-loop frequencies. That is, feedback controllers primarily add system damping. See Table 1.)

Plots of node 1 displacements and accuator inputs for cases I–IX are qualitatively all very similar to Figs. 3 and 4. Initial node 1 displacements (see Table 1) differ since $x_0(\xi)$ depends on ξ. Note that the initial displacements for the optimized structures are less than the corresponding baseline values. The same is true for nodes 2, 3, and 4. Reduced initial displacements account, at least in part, for reduced $x_0^TPx_0$ values. Figures 5–8 give node 1 displacements and control inputs for cases III and VI. Though initial node 1 displacements for excitations $x_0^1(\xi)$ exceed those for $x_0^2(\xi)$ in cases I–VI, settling times are approximately equal in all cases (about .4 s). Maximum accuator inputs at node 1 are also compared in Table 1.

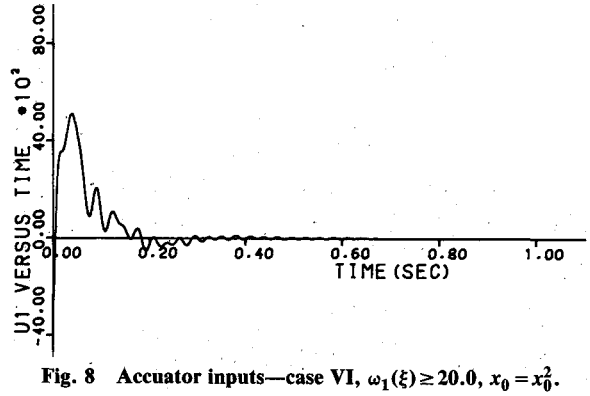

Fig. 8 Accuator inputs—case VI, $\omega_1(\xi)\geq 20.0$, $x_0=x_0^2$.

For case VII, with $x_0=x_0^1$, plots of node 1 displacements and accuator inputs are again essentially identical to Figs. 3 and 4, the major difference being that initial node 1 displacement has increased from 18.9 to 19.2 in., and maximum accuator input has decreased from 7900 to 7500 lb. Thus, the controlled dynamic response of the optimized truss is essentially equivalent to that of the baseline truss. This strongly suggests that if one's major concern is the minimization of structural mass, structural optimization on mass alone may well result in a design with largely unchanged controlled dynamic response characteristics. Such an optimization is much easier computationally than the minimization of J. Furthermore, it accomodates imposed constraints nicely, while J does not.

The dynamic response plots discussed reveal that the matrices in Eq. (15) provide effective truss control essentially independent of the combined structural and control optimization process. Interestingly, it is shown in Ref. 9 that if the optimization algorithm is applied to cases I–IX with $Q=1000\cdot I$ and $R=I$ (I an identity matrix), data strikingly similar to that listed in Table 1 result. Furthermore, corresponding dynamic response plots are practically identical to those described here.

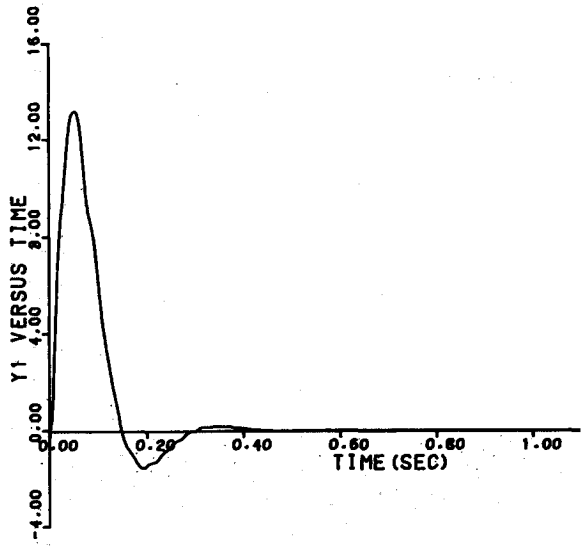

Fig. 9 Node 1 displacements—case XVI, $\alpha \cdot \delta(t)$ exerted at node 3, $\alpha = 6{,}000$.

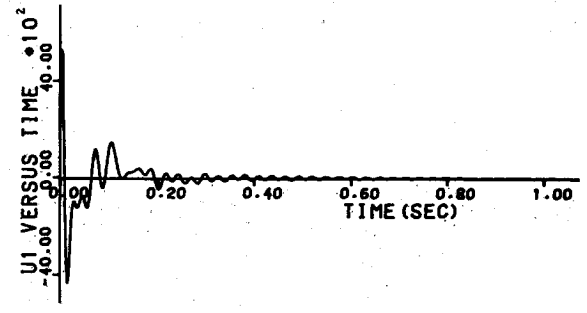

Fig. 10 Accuator inputs—case XVI, $\alpha \cdot \delta(t)$ exerted at node 3, $\alpha = 6{,}000$.

VIII. Further Optimization Results

In this section, we briefly discuss further aspects of the combined structural and control optimization problem. More thorough discussions are found in Ref. 9. We first investigate the effectiveness of optimal truss designs determined through x_0^1 in damping out the excitation x_0^2 (and vice versa). Data for cases X and XII in Table 2 was generated by exciting the optimal truss designs of cases I and III with $x_0 = x_0^2(\xi)$. In cases XI and XIII, the trusses of cases II and IV were excited with $x_0 = x_0^1(\xi)$. In Table 2, changes in W and $x_0^T P x_0$ are again measured with respect to the baseline ($\xi_i \equiv .1$) design. For cases X–XIII, changes in W are of course the same as those shown in Table 1 for corresponding designs. However, the values of $x_0^T P x_0$ have increased significantly. For example, when the truss of case I is excited by x_0^1, $x_0^T P x_0$ decreases 24%. When the same truss is excited by x_0^2, $x_0^T P x_0$ decreases only 4.6%. In cases XI and XII, $x_0^T P x_0$ actually exceeds its baseline values. This data clearly illustrates that a truss design that is optimal for one initial condition may represent, from an energy standpoint, a much poorer design for other initial excitations. Plots of node 1 displacements and accuator inputs for cases X–XIII are qualitatively quite similar to Figs. 3 and 4. Basically, only changes in initial displacements and maximum accuator inputs, respectively, are observed.

In cases XIV and XV, the optimal ξ_i values from cases III and IV are averaged for each i. It is hoped that the single resulting truss design will give rise to significant reductions in both mass and system energy developed when the truss is excited by either x_0^1 *or* x_0^2. The $x_0^T P x_0$ values for these cases show a marked improvement over the corresponding data for cases XII and XIII. However, these reductions are not as large as those observed in cases III and IV. Reductions in W are comparable in all cases. The data suggests that the averaged ξ_i values will produce favorable reductions in $x_0^T P x_0$ for any excitation x_0 that is a linear combination of x_0^1 and x_0^2. This further suggests that if one can identify a finite collection of fundamental excitations x_0^i that generate an envelope of expected system excitations, an averaging scheme applied to individually optimal designs, like the one employed here, may give rise to a single satisfactory "improved" design. Natural candidates for fundamental excitations x_0^i are truss mode shapes. One is concerned, however, that as the class of expected excitations grows, the averaging of designs may eliminate altogether reductions in energy realized with individual excitations x_0^i.

Consider now structural excitations resulting from sharp blows delivered to the structure by external agents (e.g., meteorite collisions or shuttle docking impacts). As is customary, we model these excitations as impulse forces $\alpha \cdot \delta(t)$ (delta function with magnitude $\alpha > 0$) applied to the structure. Such forces give rise to initial conditions x_0 containing zero displacements and nonzero instantaneous velocities. In the 10-bar truss, if $\alpha \cdot \delta(t)$ acts in the upward direction at node 3, for example, $x_0 = B[0\ 0\ \alpha\ 0]^T$. Note that again $x_0 = x_0(\xi)$ depends on ξ through $B = B(\xi)$. With respect to minimizing J, these initial conditions are very attractive since they are easy to calculate. Observe that in order to determine x_0 in Sec. VI, it was necessary to solve the static displacement equations $Kr_0 = B_0 f$ where $f = [f_1\ f_2\ f_3\ f_4]^T$ and f_i is the force (loading) acting at node 1.

As in Sec. VI, when initial conditions $x_0(\xi)$ are determined by impulse forces, the combined structural and control optimization problem is nicely behaved. Data for two sample cases is given in Table 2. In case XVI, an impulse force with $\alpha = 6000$ is applied to node 3 and J is minimized without constraints. The q_1 value producing the best simultaneous reduction of W and $x_0^T P x_0$ is $q_1 = 15{,}000$. For this case, W, $x_0^T P x_0$, and J all decrease roughly 9% from their corresponding baseline values (determined by exciting the $\xi_i^0 \equiv 0.1$ truss with the same impulse force). In case XVII, $\alpha \cdot \delta(t)$ with $\alpha = 2{,}000$ is applied at node 2. Here the optimal q_1 value is $q_1 = 4000$ and W, $x_0^T P x_0$, and J decrease 11.6%, 6.8%, and 8.8%, respectively. Note that the percentage decreases in performance are smaller here than in cases I and II. This is probably because $\alpha \cdot \delta(t)$ excites higher system modes than do x_0^1 or x_0^2. Further evidence of this is recorded in Figs. 9 and 10, where node 1 displacements and accurator inputs for case XVI are plotted. Observe the higher-frequency transients present in both figures.

IX. Conclusion

This paper has presented an applications-oriented strategy for solving a problem in combined structural and control optimization for flexible systems. The strategy centers around the gradient-based optimization of a cost functional depending on structural parameters alone. The need for costly second-derivative calculations is thereby eliminated. A practical optimization algorithm was outlined, its application based upon linking finite-element, optimal control, and gradient optimization software. Posed in this general setting, the algorithm applies straightforwardly to any structure with an available finite-element model.

The combined optimization problem for the 10-bar truss was solved for several cases. Initial loadings exciting first and second truss modes were considered. Significant simultaneous reductions in mass *and* energy were recorded. Two specific undesirable characteristics of the optimization problem were observed: 1) the optimal truss designs were directly dependent on selected initial conditions, and 2) the use of penalty functions to satisfy imposed constraints proved numerically unsatisfactory. Favorable characteristics observed included these: 1) eigenvalue monotonicity eliminated the need for penalty functions when fundamental frequency constraints were imposed, 2) bothersome local minima were absent, 3)

dynamic response plots revealed effective control in all optimized models, and 4) the averaging of structural designs, each optimal for a member of a class of fundamental excitations, showed promise in reducing the effects of problem initial condition dependence.

The analysis presented here has shown that the application of gradient searches to solve the combined structural and control optimization problem is feasible for structures described by general finite-element models. Numerically, the algorithm requires significant amounts of computer time, however (typically 7–15 CPU min on an IBM 3010 were required for each of the cases considered here). For high-dimensional systems, the algorithm will surely require the computational power of super computers, but its performance should be satisfactory. The major problem for the analysis lies then in the very nature of the problem itself—the fact that optimal designs are initial condition-dependent. If few modes participate in a system's dynamic response to expected excitations, it seems likely that useful results can be generated by the technique discussed here. If many modes participate however, the outcome seems less certain.

Acknowledgments

The authors would like to thank Dr. Vipperla V. Venkayya and Dr. William R. Wells for many helpful technical discussions that eventually led to our interest in the problem discussed here. Thanks also are due the referees for their careful reading and helpful suggestions. This research was sponsored by the Flight Dynamics Laboratory, Wright Patterson AFB, Dayton, OH, under Contract F33615-84-C-3217.

References

[1] *Proceedings of the Second AFOSR/NASA Forum on Space Structures*, June 11–13, 1984, Washington, D.C., edited by A. K. Amos and W. L. Hallauer Jr.

[2] Hale, A. L. and Lisowski, R. J., "Optimal Simultaneous Structural and Control Design of Maneuvering Flexible Spacecraft," *Proceedings of the Fourth VPI & SU/AIAA Symposium on Dynamics and Control of Large Structures*, Blacksburg, VA, June 6–8, 1983.

[3] Hale, A. L., Lisowski, R. J., and Dahl, W. E., "Optimizing Both the Structure and the Control of Maneuvering Flexible Spacecraft," AIAA Paper 83-377, presented at AAS/AIAA Astrodynamics Conference, Lake Placid, NY, Aug. 22–25, 1983.

[4] Hale, A. L., Lisowski, R. J., and Dahl, W. E., "Optimal Simultaneous Structural and Control Design of Maneuvering Flexible Spacecraft," *Journal of Guidance, Control, and Dynamics*, Vol. 8, 1984, pp. 86–93.

[5] Junkins, J. L., Bodden, D. S., and Kamat, M.P., "An Eigenvalue Optimization Approach For Feedback Control of Flexible Structures," *Proceedings of Southeastern Conference on Theoretical and Applied Mechanics XII*, May 10–11, 1984, Calloway Gardens, GA.

[6] Bodden, D. S. and Junkins, J. L., "Eigenvalue Optimization Algorithms for Structural/Controller Design Iterations," presented at the 1984 American Control Conference, June 6–8, 1984, San Diego, CA.

[7] Messac, A. and Turner, J., "Dual Structural-Control Optimization of Large Space Structures," presented at AIAA Dynamics Specialist Conference, Palm Springs, CA, May 17–18, 1984.

[8] Messac, A. and Turner, J., "Optimal Minimum-Mass Structural-Control Design for Large Space Structures," presented at AIAA Dynamics Specialist Conference, Palm Springs, CA, May 17–18, 1984.

[9] Miller, D. F. and Shim, J., "Combined Structural and Control Optimization for Flexible Systems Using Gradient Based Searches," AIAA Paper 86-0178, Reno, NV, Jan. 1986.

[10] Salama, M., Hamidi, M., and Demsetz, L., "Optimization of Controlled Structures," *Proceedings of Workshop on Identification and Control of Flexible Space Structures*, June 4–6, 1984, San Diego, CA.

[11] Venkayya, V. B. and Tischler, V. A., "Frequency Control and Its Effect on the Dynamic Response of Flexible Structures," *AIAA Journal*, Vol. 23, Nov. 1985, pp. 1768–1774.

[12] Fox, R. L. and Kapoor, M. P., "Rates of Change of Eigenvalues and Eigenvectors," *AIAA Journal*, Vol. 6, Dec. 1968, pp. 2426–2429.